

Supporting Information

Achieving High Quality Factor Interband Nanoplasmonics in the Deep Ultraviolet Spectrum via Mode Hybridization

Evelin Csányi^{1,2,†}, Yan Liu^{1,3,†}, Dan Kai^{1,4}, Sigit Sugiarto⁴, Henry Yit Loong Lee^{1,3}, Febiana Tjiptoharsono¹, Qifeng Ruan⁵, Soroosh Daqiqeh Rezaei⁵, Xiao Chi⁶, Andrivo Rusydi^{6,7}, Graham Leggett², Joel K. W. Yang^{5,*} and Zhaogang Dong^{1,3,5,*}

¹Institute of Materials Research and Engineering (IMRE), Agency for Science, Technology and Research (A*STAR), 2 Fusionopolis Way, Innovis #08-03, Singapore 138634, Republic of Singapore

²Department of Chemistry, University of Sheffield, Brook Hill, Sheffield S3 7HF, United Kingdom

³Quantum Innovation Centre (Q.InC), Agency for Science Technology and Research (A*STAR), 2 Fusionopolis Way, Innovis #08-03, Singapore 138634, Republic of Singapore

⁴Institute of Sustainability for Chemicals, Energy and Environment (ISCE²), Agency for Science, Technology and Research (A*STAR), 1 Pesek Road, 627833, Singapore

⁵Singapore University of Technology and Design, 8 Somapah Road, 487372, Singapore

⁶Singapore Synchrotron Light Source (SSLS), National University of Singapore, 5 Research Link, 117603, Singapore

⁷Department of Physics, 2 Science Drive 3, National University of Singapore, 117542, Singapore

[†]These authors equally contribute to this work.

*Correspondence and requests for materials should be addressed to Z.D. (email: zhaogang_dong@sutd.edu.sg), and J.Y. (email: joel_yang@sutd.edu.sg).

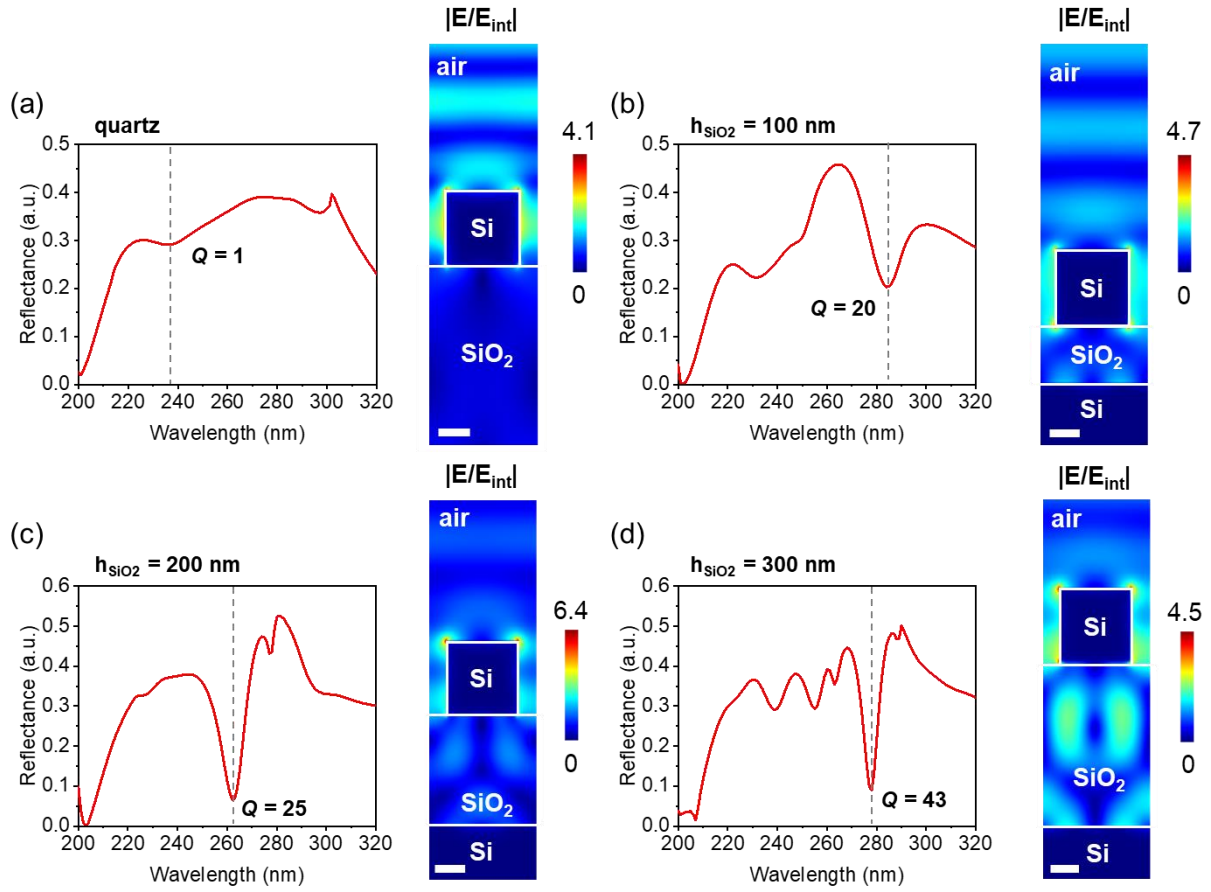


Figure S1. Simulated reflectance spectra using finite-domain-time-difference (FDTD) calculations for a nanodisk array with $h_{Si} = 130$ nm, $d = 130$ nm and $p = 200$ nm on (a) quartz and when the SiO_2 waveguide layer thickness (h_{SiO_2}) is (b) 100 nm, (c) 200 nm and (d) 300 nm. Scale bar corresponds to 50 nm.

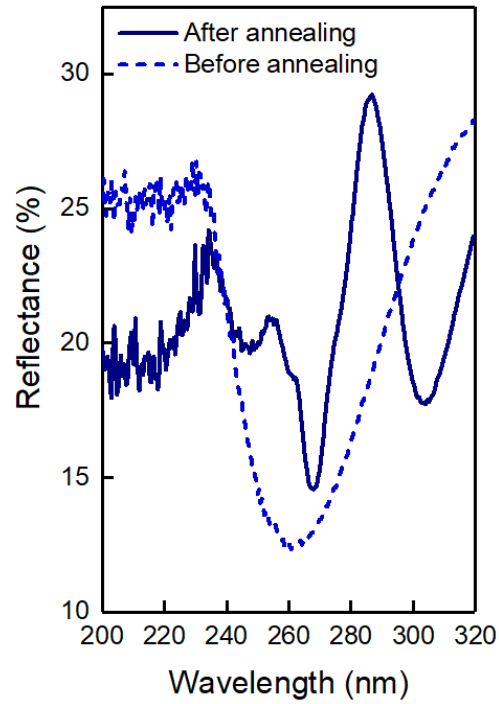


Figure S2. Experimental reflectance spectra for the Si nanohole array with $h_{Si} = 130$ nm and $d = 150$ nm, before and after the annealing process, illustrating the difference in reflectance when switching from amorphous to crystalline states of the Si.

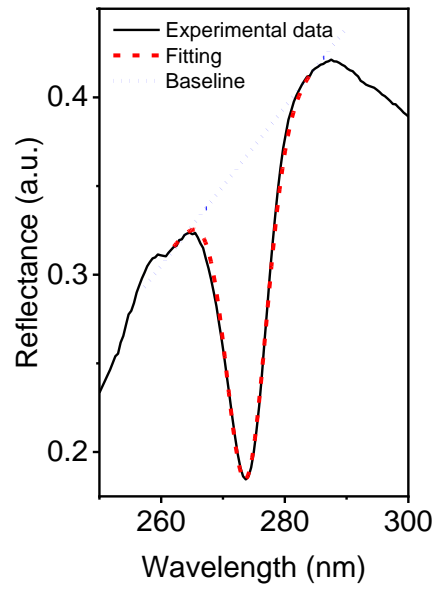


Figure S3. Experimental reflectance spectra for the nanodisk array with $h_{Si} = 130$ nm, $d = 130$ nm, $p = 200$ nm and SiO_2 layer thickness of 300 nm. The resonance dip was fitted using a standard Gaussian function, with the background manually defined. A full-width-at-half-maximum (FWHM) of 7.4 nm was obtained, with a peak centered at 273.8 nm, corresponding to a Q-factor of 37. The R^2 of the fitting is 0.998.

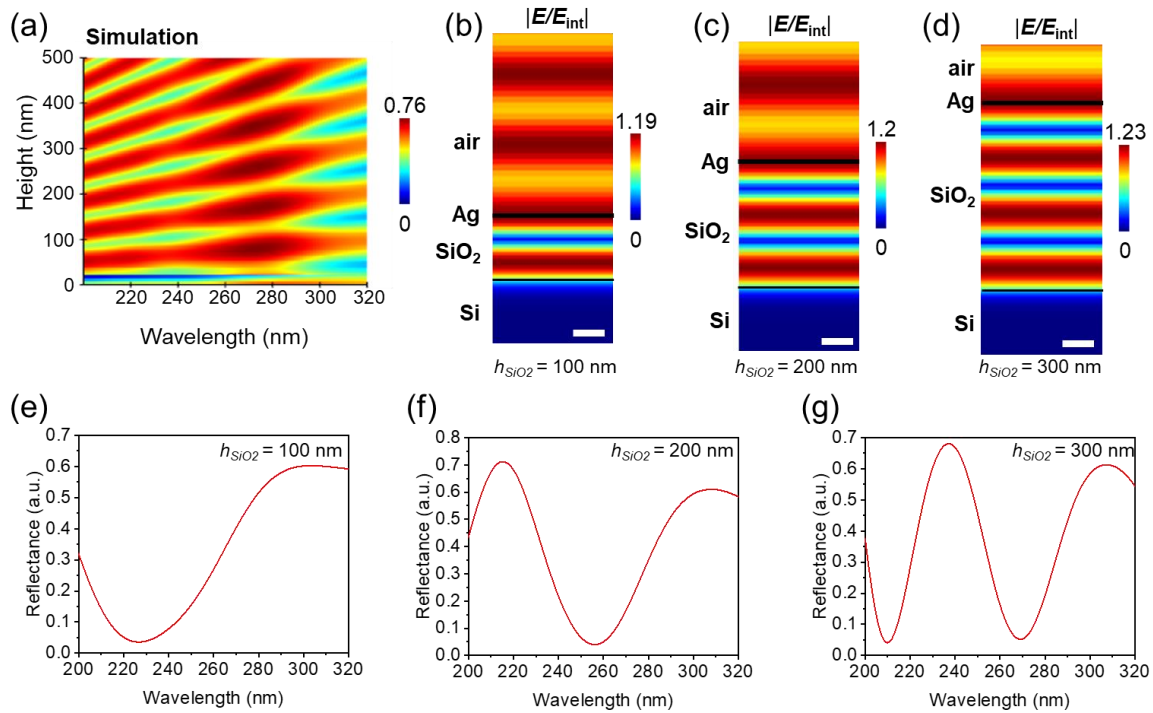


Figure S4. (a) Simulated reflectance spectra of a Si substrate with varying thickness of SiO₂ overlayer and a 15 nm Ag thin film on top. Spatial distribution of the electric field $|E/E_{\text{int}}|$ at (b) $\lambda = 227$ nm and a 100-nm-thick SiO₂ spacer layer, (c) $\lambda = 256$ nm and 200-nm spacer, (d) $\lambda = 267$ nm and a 300-nm spacer. The corresponding simulated reflectance spectra can be seen in (e), (f) and (g), respectively. **The scale bar denotes 50 nm.**

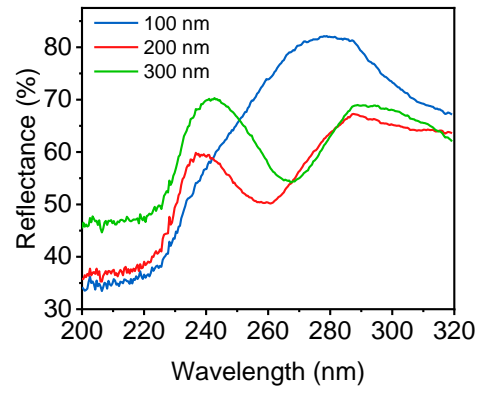


Figure S5. Experimental reflectance spectra of the silicon substrate with an overlayer SiO_2 that has a thickness of 100 nm, 200 nm and 300 nm.

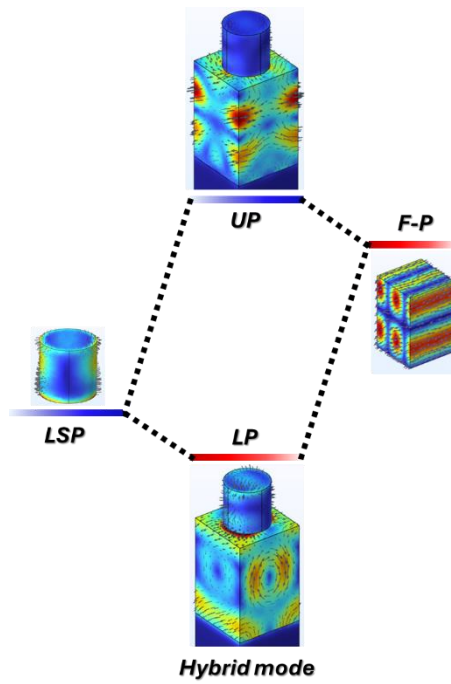


Figure S6. Hybridization of c-Si IBP mode in nanodisk and F-P mode, which yields two hybrid modes, UP mode and LP mode. It shows stronger electric field interaction in LP mode between LSP and F-P along the vertical direction than the one in UP mode.

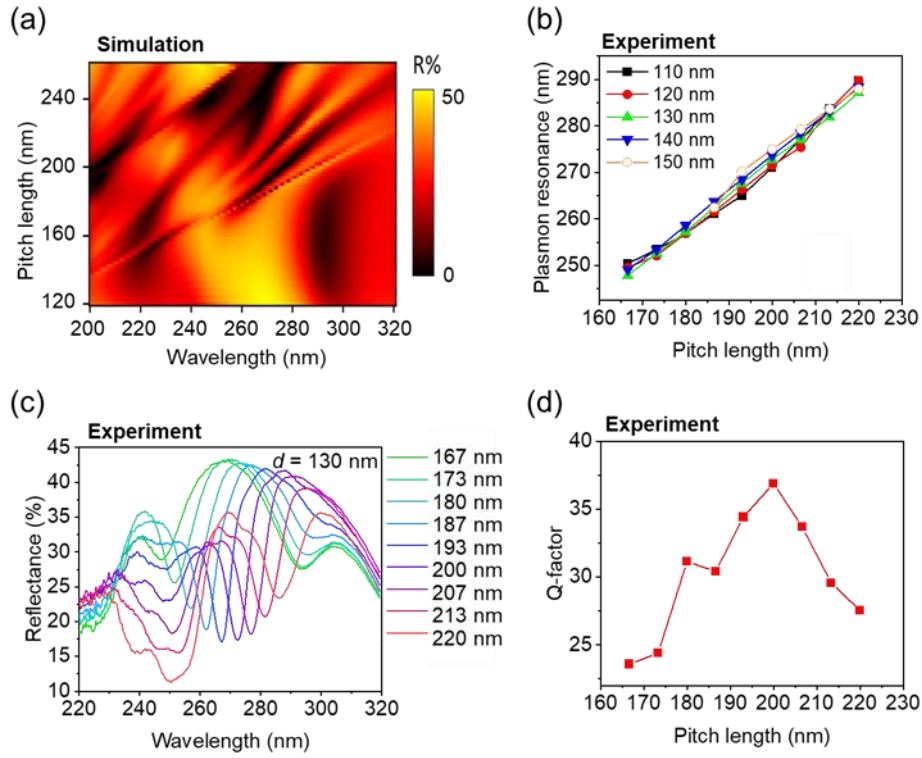


Figure S7. (a) Simulated reflectance spectra of the nanodisk array with $h_{Si} = 130$ nm, $h_{SiO_2} = 300$ nm and $d = 130$ nm as a function of the pitch length. (b) Experimental results of the spectral position of the plasmon resonance dip as a function of the pitch length for arrays with varying diameters from 110 nm to 150 nm, extracted from the reflectance measurements. (c) Reflectance spectra of arrays with $h_{Si} = 130$ nm, $h_{SiO_2} = 300$ nm and $d = 130$ nm, using varying pitch lengths and (d) the corresponding Q-factor of the resonance dips.

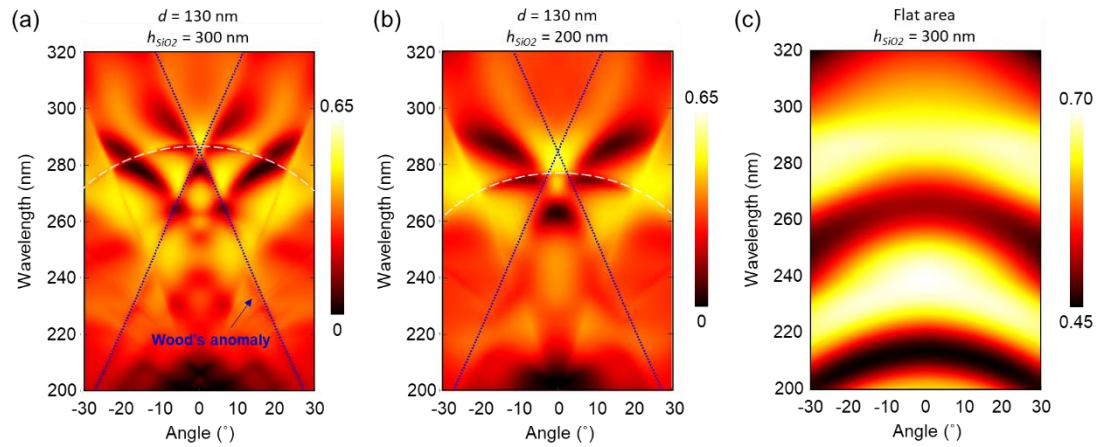


Figure S8. Simulated angle-resolved reflectance of arrays with $h_{Si} = 130$ nm, $p = 200$ nm, $d = 130$ nm and (a) SiO_2 cavity thicknesses of $h_{SiO_2} = 300$ nm and (b) $h_{SiO_2} = 200$ nm. (c) Shows the angle-resolved reflectance of the flat area without the nanoarrays when $h_{SiO_2} = 300$ nm. The blue lines represent the first order Wood's anomaly diffraction line, while the white dashed line shows the position of the feature resulting from the interference of the bare cavity and the nano-resonator modes.

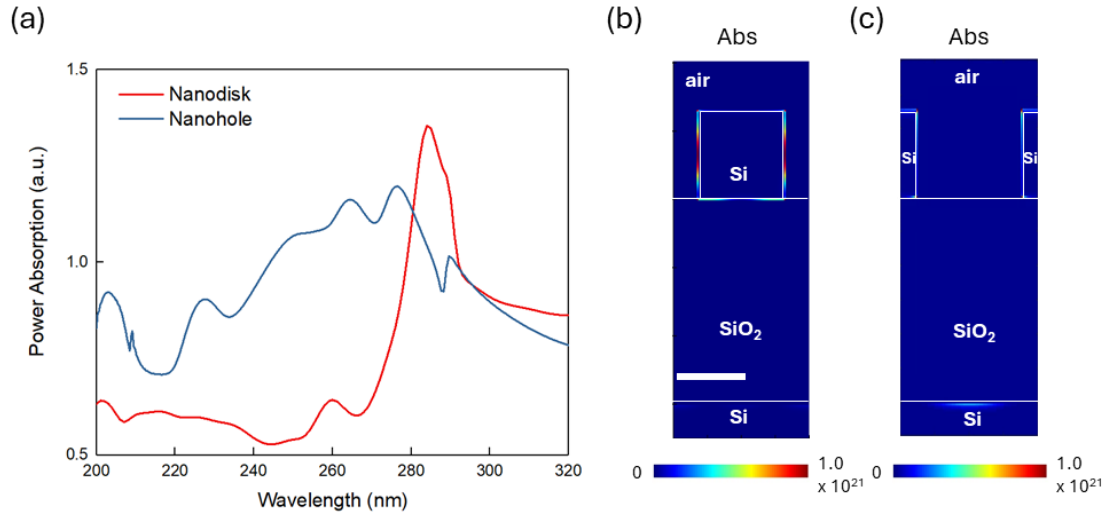


Figure S9. Simulated power absorption of nanodisk array with $h_{Si} = 130$ nm, $p = 200$ nm, $d = 130$ nm and $h_{SiO_2} = 300$ nm and nanohole array with $h_{Si} = 130$ nm, $p = 200$ nm, $d = 150$ nm and $h_{SiO_2} = 300$ nm. (a) The total power absorption of nanodisk and nanohole array. (b) The special distribution of power absorption of nanodisk at the wavelength of 278 nm. (c) The special distribution of power absorption of nanohole at the wavelength of 278 nm. The scale bar denotes 100 nm.

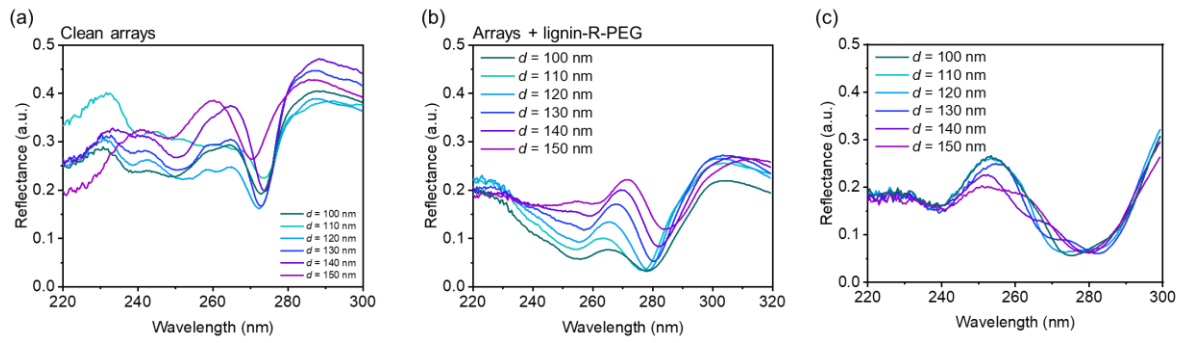


Figure S11. Experimental reflectance spectra of silicon nanodisk arrays before and after lignin-PEG. The antenna array has a $h_{Si} = 130$ nm, $p = 200$ nm and $h_{SiO_2} = 300$ nm, while varying the diameter from $d = 100$ nm to $d = 150$ nm when the surface is (a) clean, without any lignin-PEG polymer and after coating with (b) 55 nm and (c) 70 nm lignin-PEG.

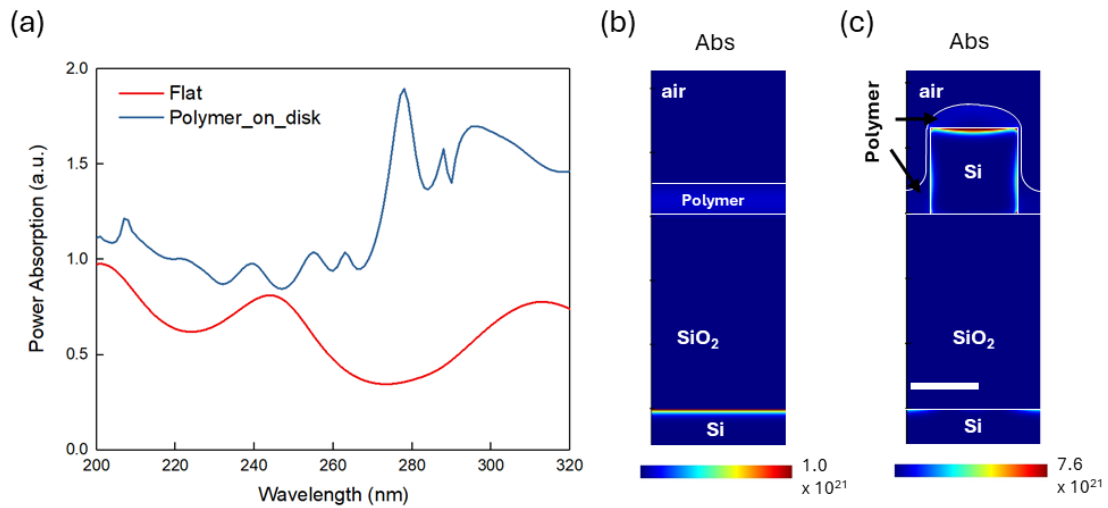


Figure S12. Simulated power absorption of lignin-PEG polymer film on the flat substrate region and silicon nanodisk array. (a) The total power absorption spectra of lignin-PEG polymer film on flat substrate region and nanodisk array. At the peak absorption wavelength 278 nm, the hybrid polymer-silicon cavity is having 5.4-fold enhanced absorption as compared to the flat substrate case. (b)-(c) Spatial distributions of power absorption for 55-nm-thick lignin-PEG polymer film on flat substrate region and silicon nanodisk array at 278 nm. The scale bar denotes 100 nm.

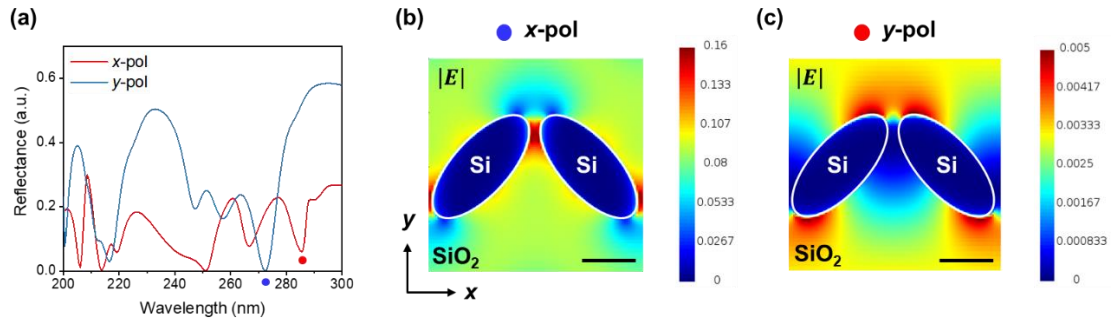


Figure S13. Polarization dependent DUV metasurface. (a) Simulated reflectance spectra for an c-Si elliptical nanodisk array with disk height of 130 nm, pitch of 200 nm on a 300-nm-thick SiO₂ spacer layer. The elliptical disks have a short axis of 50 nm and a long axis of 120 nm, with a 45° tilt introduced along the *z*-axis to break symmetry in the design. Reflectance simulations were performed under *x*-polarized and *y*-polarized incident light. (b) Corresponding electric field intensity ($|E|$) distributions at the resonance wavelengths for *x*-polarized (blue dot) and (c) *y*-polarized (red dot) light, respectively.

Methods

Si nanoarray fabrication. Pre-cleaned silicon wafers with 100 nm, 200 nm or 300 nm thick SiO₂ dielectric spacer layers (purchased from Silicon Valley Microelectronics, Inc) were used as substrates. The fabrication of reference arrays on quartz substrates followed the same experimental procedures. Thicker SiO₂ overlayers were achieved by additional SiO₂ growth using plasma-enhanced chemical vapour deposition (PE-CVD, Oxford Instruments Plasmalab System 380). The process was carried out using gases of SiH₄ at a flow rate of 7.5 sccm (standard-cubic-centimeters-per-minute) and N₂O at 20 sccm at 250 °C and under a pressure of 4.0 mTorr. A DC power of 20 watts and coil power of 1000 watts were used. Next, the substrate with SiO₂ layer was used to grow a further layer of amorphous silicon (a-Si, thickness of 75 nm or 130 nm) on top using plasma-enhanced chemical vapour deposition (PE-CVD, Oxford Instruments Plasmalab System 380). The a-Si film was grown using SiH₄ at a flow rate of 45 sccm and Ar at 30 sccm at 250 °C and 8.0 mTorr pressure, with a DC power of 50 watts and coil power of 30 watts. Next, the resulting samples were spin-coated at 5k round-per-minute (rpm) with 2% hydrogen silsesquioxane (HSQ, Dow Corning XR-1541 E-beam resist), followed directly by nanopatterning via electron beam lithography (EBL, Elionix ELS-7000). The EBL process was carried out using an electron acceleration voltage of 100 keV, beam current of 500 pA, and the exposure dose of 20,480 μC/cm² for arrays with disk diameters of 70 nm to 100 nm and 8,960 mC/cm² for diameters of 110 nm to 180 nm. Upon completion, the sample was transferred into a solution of NaOH/NaCl (1% wt./4% wt. in de-ionized water) for 60 seconds for development, followed by immersion in de-ionized water for 60 seconds. Then, the sample was rinsed by acetone, isopropyl alcohol (IPA) and dried by a continuous flow of N₂ for 1 minute. Following, the a-Si layer was etched (with over-etching of 15 nm) by inductively-coupled-plasma (ICP, Oxford Instruments Plasmalab System 100) using an ICP power of 300 watts, an RF power of 100 watts, Cl₂ flow rate of 22 sccm (standard-cubic-

centimeters-per-minute), a process pressure of 5 mTorr, and a cooling temperature of 10 °C. Lastly, the samples were annealed using rapid thermal annealing (Jipelec, Jetfirst rapid thermal processing system) under nitrogen flow of 1500 sscm, a temperature ramp rate of 14.2 °C/s over 60 s and annealed at 850 °C for 120 s. Controlled cooling to room temperature over a period 300 s yielded the final arrays with crystalline silicon (*c-Si*) patterns.

Synthesis and coating of lignin-poly(ethylene glycol) (lignin-PEG). Lignin-PEG copolymer was synthesized *via* Reversible Addition Fragmentation Chain Transfer (RAFT) polymerization.³⁸ For the synthesis of lignin-RAFT macroinitiator, alkali lignin (AL, Sigma Aldrich) was dried overnight at 105 °C to remove any excess moisture in lignin for the synthesis. Oven dried alkali lignin (3.0 g, 1 eq.), RAFT chain transfer agent (CTA), (S)-4-cyano-4-[(dodecylsulfanylthiocarbonyl)sulfanyl]pentanoic acid (2.4 g, 10 eq.) and N,N-dicyclohexylcarboimide (DCC) (1.5 g, 12 eq.) were added to an oven dried round bottom flask. The reaction flask was flushed with argon to allow an inert atmosphere. Anhydrous dimethylformamide (DMF) (50 mL) and catalytic amount of N,N-dimethylaminopyridine (DMAP) were then introduced into the flask under argon. The reaction mixture was stirred at 300 rpm at room temperature for 24 h. The crude product was purified via precipitation in diethyl ether with a yield of 54.0%. The product was a dark brown powder. For the synthesis of lignin-PEG, synthesised lignin-RAFT macroinitiator (0.5 g, 1 eq.), poly(ethylene glycol) methacrylate ($M_n = 950$ Da, 5.0 g, 100 eq.), VAZO-88 initiator (2.0 mg, <0.1 eq.), and anhydrous DMF (30 mL) were added to an oven dried Schlenk flask. Using liquid nitrogen, three cycles of freeze-evacuate-thaw was systematically performed to degas the system. The reaction flask was stirred at 300 rpm at 90°C, under argon atmosphere for 48 h. The crude product was precipitated in diethyl ether: hexane (1: 9) precipitating solvent, twice, to obtain a viscous dark brown liquid. The characterization of the resulting polymer can be found in Figure

S10. For the coating of the nanoarray substrates, the lignin-PEG was dissolved in tetrahydrofuran (THF, 10 mL/mg). The samples were first treated using inductively-coupled plasma (Oxford Plasmalab System 80) at an O₂ flow rate of 50 sccm. The DC power used 100 watts, a coil power of 500 watts, a process pressure of 10 mTorr at room temperature. Next, the samples were spin-coated with the lignin-PEG solution (10 mL/mg, THF). Film thicknesses of ~55 nm and 70 nm were achieved using a spin-coating speed of 5k rpm and 2k rpm respectively.

Optical, ellipsometry and SEM characterizations. The optical constants of the lignin-modified poly(ethylene glycol) films were measured via spectroscopic ellipsometry at 50 °, 60 ° and 70 ° incident angles across the 190 nm to 320 nm spectral region. Optical reflectance measurements of the samples were taken using a CRAIC UV-VIS-NIR microspectrophotometer and a Zeiss Ultrafluar objective (×10 objective lens with a numerical aperture of 0.2), with a polarized broadband light source. Calibration for the absolute reflectance spectra was achieved using a NIST traceable calibration sample from CRAIC Technologies (<http://www.microspectra.com/>). The measurements were taken using an aperture size of 72 μm × 72 μm and integration time of 100 ms, where 50 measurements were averaged so as to reduce the measurement noise. The scanning electron microscope (SEM) images were taken with an electron acceleration voltage of 5 kV (Elionix, ESM-9000). Prior to the SEM imaging, the samples were coated with 5 nm of Cr using electron beam evaporation (Denton Explorer E-beam Evaporator) to reduce the anomalous contrast due to charging. A deposition rate of 1 Å/s at a pressure of 4 × 10⁻⁶ Torr was used for the Cr layer deposition.

Numerical Simulations. Three-dimensional finite-difference time-domain (3D-FDTD) simulations were carried out to obtain the far field spectra and the near-field distributions using

Lumerical FDTD Solutions software. The simulated unit cell with a dimension of $200\text{ nm} \times 200\text{ nm} \times 1200\text{ nm}$ with perfectly matched layer (PML) for the z direction and periodic boundary conditions for the x and y directions at normal incidence condition. A plane wave source was used, with a monitor placed above the source to record the reflectance spectrum. The mesh size was set to be $2\text{ nm} \times 2\text{ nm} \times 2\text{ nm}$. The material properties of Si were chosen based on the optical dielectric constants taken from previous measurements. For the lignin-PEG film, the refractive index (n) and extinction coefficient (k) values obtained from the spectroscopic ellipsometry were applied, while the optical dielectric constant of the SiO_2 cavity was taken from the software's material database as adapted from Palik.¹ The electric, magnetic, and charge field distributions were collected, as well as the total power absorption. To study the angle-dependent reflectance, a broadband fixed angle source technique (BFAST) plane wave was used to provide broadband simulations at a range of illumination angles. Multipolar decomposition analysis was carried out using COMSOL Multiphysics software, performing finite-element method (FEM) simulations. The details of the simulation setup were outlined by Dong et al.²

(1) Palik, E. D. Preface. In *Handbook of Optical Constants of Solids*, Palik, E. D. Ed.; Academic Press, 1997; pp xvii-xviii.

(2) Dong, Z.; Ho, J.; Yu, Y. F.; Fu, Y. H.; Paniagua-Dominguez, R.; Wang, S.; Kuznetsov, A. I.; Yang, J. K. W. Printing Beyond sRGB Color Gamut by Mimicking Silicon Nanostructures in Free-Space. *Nano Letters* **2017**, *17* (12), 7620-7628.